Integration of solar field into a combined cycle power plant for fuel saving in insular subtropical climates

Adham M Abdelhalim[a], Andrés Meana-Fernández[b], Ines Suarez-Ramon[c]

[a] Mechanical Engineering Department, College of Engineering and Technology, Arab Academy for Science, Technology and Maritime Transport, Alexandria, Egypt, adhammuhamed90@aast.edu
[b,c] Thermal Machines and Engines Area, Department of Energy, University of Oviedo, Gijon, Spain, [b]andresmf@uniovi.es (CA), [c]ines@uniovi.es

Abstract:

The harmful environmental effects of fossil fuels and the variability in their prices are shifting attention away from conventional combined cycle power plants. Supply issues in islands are also a problem to be considered. The objective of this work is to evaluate the feasibility of integrating solar energy into a combined cycle power plant for fuel saving in insular subtropical climates. With this aim, a case study comprising a 93 MW combined cycle in Las Palmas de Gran Canaria (Spain) and the integration of solar energy in the gas upper cycle has been presented and analyzed with a thermodynamic model. The effects of incorporating solar heat before and after the cycle compressor were assessed, finding that injecting 35 MW of solar heat before the compressor resulted in savings of 49% of the original fuel consumption and an increase of 2% in the global cycle efficiency, but at the expense of reducing the net power delivered by 47%. On the other hand, incorporating the solar heat after the compression process resulted in an overall 16.2% increase in the cycle efficiency, while delivering the same net power as the original cycle and reducing fuel consumption in 22%. With the increase in the amount of solar heat added to the cycle, the difference between both options became greater, with the best option being injecting solar heat after the compressor. Estimations of the economic and environmental effects of the most suitable option are provided, resulting in potential overall savings of 7.14 million Euro per year and a yearly potential of 13.75 Mkg of CO_2 emissions avoided. The results of this work are expected to contribute to improve energy supply problems by using a renewable energy source and reduce fuel imports, providing more energy stability and security to the inhabitants of islands with similar climates as Las Palmas.

Keywords:

Integrated solar combined cycle power plants (ISCCs), fuel saving, insular subtropical climate, dynamic analysis, and CO_2 emission.

1. Introduction

Nowadays, there is almost no debate on the damaging effects that global reliance on fossil fuels holds for the future of the world. Fossil fuels (e.g., coal, natural gas, and oil), apart from being finite, entail several harmful effects in the environment, especially with CO_2 emissions increasing at an alarming rate. Over the past 12 years, global CO_2 emissions from energy combustion and industrial processes have increased by 4.2 Gt CO_2, to a value of 36.8 Gt CO_2 in 2022 [1]. CO_2 emissions from natural gas combustion increased by more than 215 Mt CO_2 in 2021, to reach an all-time high of 7.35 Gt CO_2, representing 22% of the total CO_2 emissions. On the other hand, the use of renewable energy sources increased by 3% in 2020, with a prime 7% growth in renewable electricity generation. Global renewable electricity generation increased from 27% in 2019 to 29% in 2020, reaching 30% in 2021 [1]. In this context, solar energy technologies represent one of the most mature options, with its share increasing from 1.08% in 2015 to 3.74% in 2022 [2].

Integrated solar combined cycle power plants (ISCCs) are one of the most promising solar hybrid configurations for power plants. ISCCs are composed of a concentrated solar power plant (CSP) and a natural gas-fired combined cycle (NGCC). The CSP plant is normally used either to produce additional steam for the combined cycle steam turbine [3, 4], or to preheat the compressed air in the gas turbine before entering the combustion chamber [5]. It has been estimated that the CSP contribution to global energy supply may reach 3-3.6% by 2030 and 8-11.8% by 2050 [6], alongside a drop in CSP costs to $0.05/kWh by 2050. Four main technologies exist for concentrating solar power in the CSP: parabolic trough collectors, solar tower, solar dish, and linear Fresnel systems, with parabolic trough collectors (PTC) being the most mature technology. These collectors, with high thermal efficiency, high performance systems, light structures, and low-cost technology,

 https://doi.org/10.52202/069564-0055

can deliver up to 400 ºC. This temperature is generally high enough for most of industrial heating processes and applications. In addition, this technology is also suitable for low-temperature industrial applications, such as desalination and sterilization processes.

1.1. Solar integration in combined power plants and research question

The first solar plant using parabolic trough technology was built in 1913 in Maadi, Cairo, Egypt. It was built for the purpose of power generation for pumping water for irrigation [7,8]. The technology of the ISCC system was proposed by Luz Solar International [9]. During 1980s, nine solar electric generating systems (SEGS) with a total capacity of 356 MW were installed in California desert, United States, where solar collectors capture and concentrate sunlight to heat a synthetic oil (Therminol), which then heats water to generate steam [10]. SEGS became one of the most important projects that paved the way for executing subsequent similar works. In 2000, the Global Environment Facility (GEF), an organization that supports developing countries' work to address the world's most pressing environmental issues, embraced the idea of encouraging the erection of ISCC power plants in developing countries with high solar irradiation, allocating up to $50 million for the construction of four ISCCs in the Middle East. This led to an increase in the interest in CSP technologies, especially in PTCs [11]. Consequently, wide research has been performed on this technology. Some works focus on studying system integration schemes between the PTC and the combined cycle, while others analyze the static or dynamic performance of the ISCC under different conditions. In 1997, the first technical and economic analysis of the ISCC was performed in Tunisia, where the authors clarify that ISCC system is more profitable than SEGS [12]. The performance of ISCC, SEGS and Combined Cycle (CC) power plants was studied, using IPSEpro and GateCycle software [13]. After comparing the three systems, they stated that ISCC technology had the best efficiency.

In 2013, the dynamic performance of a solar Rankine cycle and ISCC was compared with the solar thermoelectric components library in TRNSYS [14]. The results showed that ISCC had higher solar-to-electric efficiency values than the solar Rankine cycle. It was also found that using solar tower technology improved annual solar-to-electric efficiency by 21.8% with respect to PTC. One year later, ISCC and the conventional CC were compared, finding many advantages with ISCC, such as peak time efficiency and less carbon dioxide emissions [15]. Several configurations of solar integration with conventional CC plants were discussed later [16]. Results show that lower stack temperatures may be achieved, allowing for a better thermal match in the heat recovery steam generator (HRSG), so more feedwater may be circulated in the cycle. In 2018, ISCC power plant was compared with a thermal storage system and a conventional CC in thermo-economic and environmental terms, using a TRNSYS dynamic simulation [17]. Overall electrical efficiency improved by 1% compared to the conventional CC. A MATLAB dynamic model for the Hassi R'mel ISCC power plant in Algeria was validated under off-design conditions, finding that some factors could affect strongly the ISCC performance, such as wind speed and direct normal irradiance (DNI) [18]. In 2021, a dynamic model was developed of an ISCC power plant in Kuraymat, Egypt, using APROS software to evaluate the ISCC performance, limitations, and capabilities, validating the results with actual operational data [19]. The model was able to reproduce most of the operating parameters, such as pressure, temperature, mass flow rates and output power. An economic and performance assessment of the ISCC-PTC system in Hassi R'mel (Algeria), coupled with a new thermal storage system was performed [20]. Results revealed that a better grid stability was reached, increasing solar energy conversion and overall performance. The net solar thermal energy conversion ratio and the energy efficiency reached 14 and 56.06%, with natural gas consumption savings representing around $30 million. Finally, in 2022, different basic ISCC system models were compared with SEGS and gas turbine combined cycles (GTCC), presenting a method for assessing ISCC systems with different integration modes and solar operating temperatures [21]. Different integration points in the steam and gas cycles, as well as two working modes, “power boosting” and “fuel saving” were discussed. For the “power boosting” mode, solar energy is injected into the steam bottom cycle to heat up the gas turbine exhaust, the live steam, the reheated steam, or the feedwater. The main idea is to keep fuel consumption constant, while the output power increases as a consequence of the increase in the steam flowrate (mas flowrate boosting) or the enthalpy increase (parameter boosting). On the other hand, the “fuel saving mode” injects the solar energy in the upper Brayton cycle, heating the compressed air before entering the combustion chamber. This leads to a decrease in the fuel mass flowrate, leaving unaffected the operating conditions in the gas turbine and thus the bottom steam cycle.

The objective of this work is to evaluate the feasibility of integrating solar energy into a combined cycle power plant for fuel saving in insular subtropical climates and estimate its effect on the energy efficiency of the cycle, fuel saving, and possible economic savings and reduction of CO_2 emissions. With this aim, a case study comprising a combined cycle in the Canary Islands (Spain) and the integration of solar energy in the gas upper cycle has been developed and analyzed with a thermodynamic model. The results are expected to contribute to improve energy supply problems by using a renewable energy source and thus reducing fuel imports, providing more energy stability and security to the island inhabitants. After briefly reviewing the energy context in the Canary Islands, the methodology followed in this work is detailed. Then, the results are discussed, and finally the main conclusions of this work are presented.

2. Case study

The geographical nature of islands enforces them to have isolated energy systems unless a connection between their electricity power grid and another grid beyond its shores is developed. This entails a series of economic and environmental difficulties. Islands are highly dependent on imported fossil fuel, leading to high costs of fuel transportation, energy supply insecurity and higher electricity prices [22]. However, renewable energy resources (solar, wind & ocean waves) often exist in abundance in islands.

2.1. The energy context in the Canary Islands

The Canary Islands are a group of seven Spanish islands that are located off the African west coast. Around 84.2% of their energy demand was supplied from non-renewable energy sources in 2022, as shown in Figure 1. Combined cycle power plants have the highest share, 44.5%, while renewable energy resources contribute only with 15.8% [23]. Figure 2 shows the solar thermal capacity installed on each island, alongside the occupied area by thermal installations. The total thermal capacity of the archipelago is 88.7 MW, being Gran Canaria Island the highest contributor, with 38.7% of the total solar thermal energy installed in the Canary.

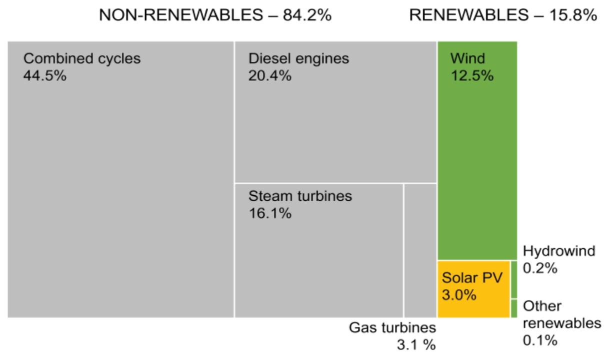

Figure 1. Canary Island electricity distribution in 2022 (Data source: [23]).

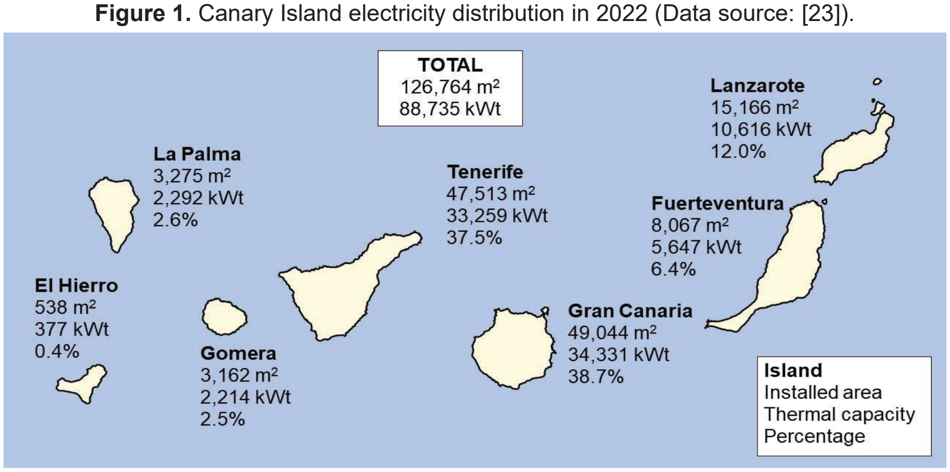

Figure 2. Installed solar thermal capacity in the Canary Islands on Dec 31st, 2021 (Data source: [24]).

The details of the energy system of the Canary Islands are collected in Table 1 [24]. The highest renewable energy sources (RES) share may be found in the island El Hierro, with 66.8%; however, this represents only 0.4% of the whole archipelago generation. The lowest RES capacity is found in La Gomera island, with only 0.4 MW. In this context, the study presented in this work may contribute to improve the energy supply network in the Canary Islands with a proposal based on renewable energy sources to integrate solar energy into existing combined cycles, providing more energy security to the islands.

2.2. ISCC in Las Palmas de Gran Canaria

The basic combined cycle power plant consists of an upper gas cycle, a bottom steam cycle, and a Heat Recovery Steam Generator (HRSG). The main characteristics of the CC, based on the power plant from Egyptian Petrochemical Company [25], with a thermal efficiency of 57.8% are shown in Table 2. In this work, two possibilities (Figures 3 &4) for the integration of the solar field within the CC, both working on a fuel saving scheme, have been studied and compared:

- Case A: solar field is integrated to preheat ambient air before the compressor inlet.
- Case B: solar field is integrated to heat up compressed air, before the combustion chamber inlet.

https://doi.org/10.52202/069564-0055

Table 1. Overview of the power system of the Canary Islands [24]

	Tenerife	Gran Canaria	Lanzarote	Fuerteventura	La Palma	La Gomera	El Hierro	Total
Total Generation (MWh)	3,710,951	3,581,933	906,078	716,839	281,016	76,850	62,430	9,336,098
Thermal Generation (MWh)	3,014,854 (81.2%)	3,028,053 (84.5%)	826,454 (91.2%)	636,732 (88.8%)	251,935 (89.7%)	76,696 (99.8%)	20,738 (33.2%)	7,855,463 (84.1%)
RES Generation (MWh)	696,097 (18.8%)	553,880 (18.8%)	79,623 (8.8%)	80,108 (11.2%)	29,081 (10.3%)	154 (0.2%)	41,692 (66.8%)	1,480,635 (15.9%)
Total Installed Capacity (MW)	1428.5	1228.4	266.8	229.8	118.4	21.6	37.8	3331.3
Thermal Capacity (MW)	1111.6 (77.58%)	1024.1 (83.4%)	232.4 (87.12%)	187 (81.4%)	105.3 (89%)	21.2 (98.1%)	14.9 (39.4%)	2696.5 (80.9%)
RES Capacity (MW)	316.9 (22.2%)	204.3 (16.6%)	34.4 (12.9%)	42.8 (18.6%)	13.1 (11%)	0.4 (1.9%)	22.9 (60.6%)	634.8 (19.1%)
CO_2 Emissions (tCO_2)	2,119,442	2,065,132	549,592	482,643	171,820	52,844	14,268	5,451,691

Table 2. Technical data for the combined cycle power plant [25]

	Compressor	
Gas cycle	Inlet Ambient temperature (ºC)	24
	Inlet pressure (bar)	1
	Isentropic efficiency (%)	97.5
	Combustion chamber	
	Inlet pressure (bar)	15.7
	Inlet temperature (ºC)	379
	Turbine	
	Inlet temperature (ºC)	1174
	Exhaust temperature (ºC)	549
	Exhaust mass flow rate (kg/s)	174.7
	Isentropic efficiency (%)	84.7
Steam cycle	Inlet steam pressure (bar)	43
	LP evaporator pressure (bar)	2.4
	Condenser pressure (bar)	0.08
	Inlet steam temperature (ºC)	452
	Pinch temperature (ºC)	18.3
	Economizer outlet temperature (ºC)	228
	Approach temperature (ºC)	26.7
	LP evaporator mass flow rate (kg/s)	5
	HP evaporator mass flow rate (kg/s)	25
Combined cycle	Total power output (MW)	93
	Cycle efficiency (%)	57.8

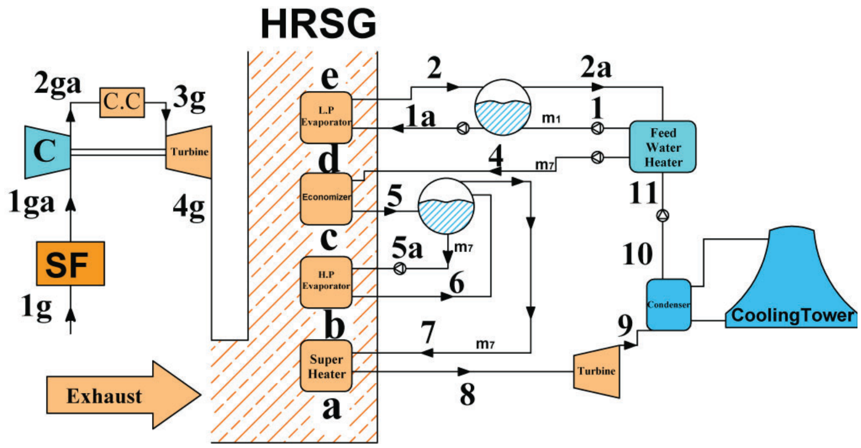

Figure 3. Case A: solar field integrated before gas cycle compressor.

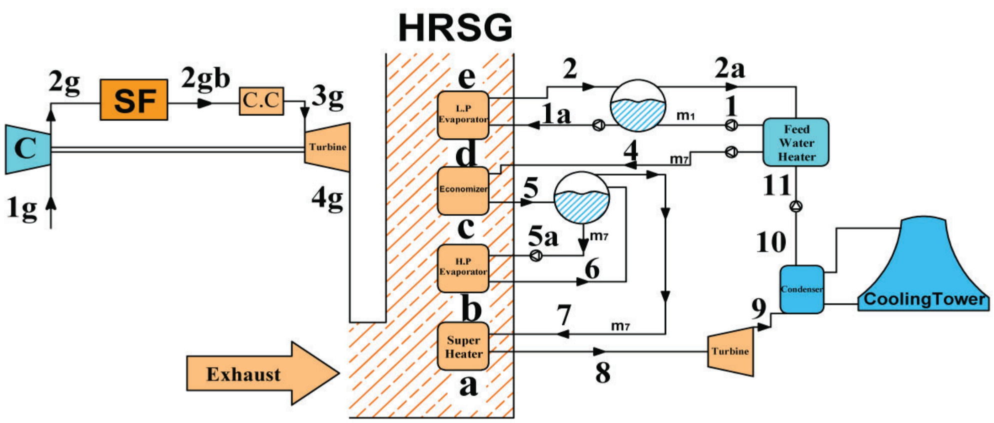

Figure 4. Case B: solar field integrated after gas cycle compressor.

3. Methodology

To fulfill the objectives of the study, a thermodynamic model has been developed in MATLAB with the Ideal Air code and the X Steam toolbox to obtain air and water properties for the upper gas and bottom steam cycles. The sequence of the methodology has been summarized in Figure 5, whereas the main thermodynamic equations used are discussed in the following subsections. A system of thermodynamic equations based on mass and energy balances in the cycle was solved, with the aim of calculating thermodynamic states, net power, efficiency, and air and fuel mass flows for the original CC and the two ISCC cases, allowing to estimate the amount of fuel saved, as well as economic savings and the reduction in CO_2 emissions. The values of solar heat integrated ranged from 0 to 35 MW. Pressure drop in the cycle was not considered, as well as the effect of inlet conditions in the isentropic efficiency of the compressor.

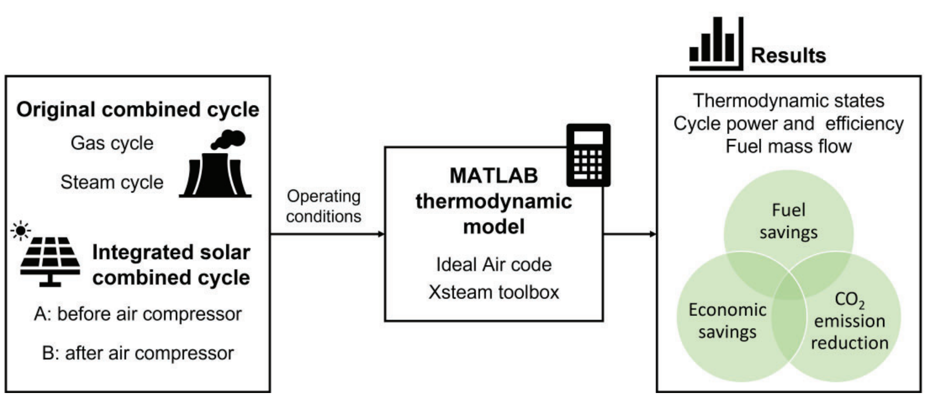

Figure 5. Methodology followed in this work.

https://doi.org/10.52202/069564-0055

3.1 Thermodynamic model of the original combined cycle

The upper gas cycle of the CC consists of three main components: compressor, combustion chamber and gas turbine. Ambient air (1g) is compressed to a higher pressure and temperature (2g). Then, it enters the combustion chamber, where fuel is added and burnt. The resulting high temperature gases (3g) enter the turbine and are expanded to ambient pressure (4g), producing useful work. Finally, exhaust gases are sent to the HRSG. The power of the gas turbine and compressor, the heat supplied in the combustion chamber and the net power of the gas cycle are calculated using the following equations:

$$\dot{W}_{GT} = \dot{m}_g \cdot \left(h_{3g} - h_{4g}\right) \tag{1}$$

$$\dot{W}_{comp} = \dot{m}_a \cdot \left(h_{2g} - h_{1g}\right) \tag{2}$$

$$\dot{Q}_{cc} = \dot{m}_f \cdot LHV = \dot{m}_g h_{3_g} - \dot{m}_a h_{2g} \tag{3}$$

$$\dot{W}_{G_{net}} = \dot{W}_{GT} - \dot{W}_{comp} \tag{4}$$

The bottom steam cycle of the CC comprises a steam turbine, a condenser, and a preheater. The steam that powers the cycle is generated in the HRSG with heat from the gas turbine exhaust gases. Energy balances in the HRSG yield the following equations (please refer to Figures 3-4 for the labels of thermodynamic states):

$$\dot{m}_g \cdot (h_a - h_b) = \dot{m}_7 \cdot (h_8 - h_7) \tag{5}$$

$$\dot{m}_g \cdot (h_b - h_c) = \dot{m}_7 \cdot (h_6 - h_{5a}) \tag{6}$$

$$\dot{m}_g \cdot (h_c - h_d) = \dot{m}_7 \cdot (h_5 - h_4) \tag{7}$$

$$\dot{m}_g \cdot (h_d - h_e) = \dot{m}_1 \cdot (h_2 - h_{1a}) \tag{8}$$

The steam turbine power is calculated as:

$$\dot{W}_{ST} = \dot{m}_7 \cdot (h_8 - h_9) \tag{9}$$

Hence, the total net power and efficiency of the CC power plant may be obtained as:

$$\dot{W}_{Total} = \dot{W}_{G_{net}} + \dot{W}_{ST} \tag{10}$$

$$\eta_{CC} = \frac{\dot{W}_{G_{net}} + \dot{W}_{ST}}{\dot{Q}_{cc}} \tag{11}$$

3.2 Thermodynamic model of the integrated solar combined cycle

The solar field has been integrated into the upper gas cycle, either to preheat ambient air before compression (case A), or to heat up compressed air before it enters the combustion chamber (case B). Gas turbine operating conditions (mass flow, inlet and outlet temperatures) are kept constant, so the steam cycle is virtually the same as the original one. In case A, the solar field generates a temperature rise before the compressor:

$$\dot{Q}_{Solar} = \dot{m}_{a_{new}} \cdot \left(h_{1gnew} - h_{1g}\right) \tag{12}$$

And the compressor power becomes:

$$\dot{W}_{comp_a} = \dot{m}_{a_{new}} \cdot \left(h_{2gnew} - h_{1gnew}\right) \tag{13}$$

On the other hand, in case B, heat is added after the compression process, leaving the compressor unaffected:

$$\dot{Q}_{Solar} = \dot{m}_{a_{new}} \cdot \left(h_{2gnew} - h_{2g}\right) \tag{14}$$

In both cases, the mass and energy balances in the combustion chamber are affected:

$$\dot{m}_g = \dot{m}_{a_{new}} + \dot{m}_{f_{new}} \tag{15}$$

$$\dot{Q}_{cc,new} = \dot{m}_{f_{new}} \cdot LHV = \dot{m}_g h_{3_g} - \dot{m}_{a_{new}} h_{2g_{new}} \tag{16}$$

And the total net power and cycle efficiency are modified accordingly, following Equations 10 and 11.

3.3 Estimation of economic and environmental effects of solar integration

Considering a natural gas price of 0.131 €/kWh [26], an estimation of the economic savings related to the amount of fuel saved may be performed using the following equation:

$$\text{Savings}_f = (\dot{m}_f - \dot{m}_{f_{new}}) \cdot LHV \cdot C_f \cdot \Delta t = \dot{m}_{f_{saved}} \cdot LHV \cdot C_f \cdot \Delta t \tag{17}$$

In addition, the introduction of solar energy reduces fuel combustion in the gas combustion chamber, leading to a reduction in CO_2 emissions. This reduction may be estimated from the lower heating value of natural gas (47,000 kJ/kg) [27] and the emission factor that relates natural gas and CO_2, 0.252 kg/kWh [28]:

$$\text{Savings}_{CO_2} = \dot{m}_{f_{saved}} \cdot LHV \cdot EF_{NG \to CO_2} \cdot \Delta t \tag{18}$$

4. Results

The results of the model show that the integration of solar heat into the combined cycle power plant results in a decrease in the fuel flow rate in cases A and B, with the air to fuel ration increasing accordingly. Table 4 collects the results from the three studied cycles when 35 MW of solar heat are added to the cycle.

Table 4. Original CC vs ISCC with 35 MW solar heat

Mass flow rates	**Original CC**	**ISCC (case A)**	**ISCC (case B)**
Air to fuel ratio	*50*	*99*	*64*
Turbine gas flow rate (kg/s)	*174.7*		
Air flow rate (kg/s)	*171.27*	*172.9*	*172.02*
Fuel flow rate (kg/s)	*3.42*	*1.74*	*2.67*
Fuel saving (%)	--	*49*	*21.83*
Operating temperatures	***Original CC***	***ISCC (case A)***	***ISCC (case B)***
Compressor inlet (ºC)	*24*	*223.6*	*24*
Combustion chamber inlet (ºC)	*379*	*785*	*565*
Gas turbine inlet (ºC)	*1174*		
Gas turbine outlet (ºC)	*549*		
Solar heat integration	***Original CC***	***ISCC (case A)***	***ISCC (case B)***
Integrated solar heat (MW)	--	*35*	
Cycle efficiency	***Original CC***	***ISCC (case A)***	***ISCC (case B)***
Gas turbine cycle (%)	*39.84*	*25.2*	*51*
Combined cycle (%)	*57.8*	*60.4*	*73.9*
Cycle power breakdown	***Original CC***	***ISCC (case A)***	***ISCC (case B)***
Compressor (kW)	*62,450*	*106,601*	*62,450*
Gas turbine (kW)	*126,727*	*126,727*	*126,727*
Gas cycle (kW)	*64,277*	*20,722*	*64,277*
Steam cycle (kW)	*28,810*	*28,810*	*28,810*
Total net power (kW)	*93,000*	*49,087*	*93,000*
Specific work per unit fuel mass flow (kJ/kg)	*27,193*	*28,211*	*34,831*
CO_2 emissions saving (kg CO_2/kWh)	-	*0.0572*	*0.0166*

Option A results in a higher amount of fuel saving, 49%, whereas option B saves around 22%. However, the compressor power required increases by 70% with option A. Considering the changes in energy efficiency, option A results in a drop in the efficiency of the gas cycle of around 14.5%, although a slight increase in the overall combined cycle of around 2% is achieved, due to the reduction of heat supplied to the combustion chamber. Option B achieves the maximum cycle efficiency increase, around 11% for the gas cycle, leading to a 16.2% increase in the efficiency of the combined cycle. Therefore, option B seems the most beneficial option, delivering the same net power to the net with a substantial reduction on fuel consumption. The specific work per unit fuel mass flow rate reflects the superiority of case B over case A as 34,831 kJ could be delivered for each kg of fuel, while only 28,211 kJ for case A. CO_2 emissions avoided per net energy production is computed, where it is found that CO_2 emissions could be saved at a rate of 0.0572 and 0.0166 kg/kWh for case A and case B respectively.

Figure 6 shows the evolution of the cycle efficiency for the ISCC options studied as a function of the integrated solar heat, from 0 to 35 MW. It may be observed that integration of solar heat always results in better cycle efficiencies if it is done as proposed in option B, with the gap between options B and A increasing with further addition of solar heat. On the other hand, considering the fuel mass flow rates, depicted in Figure 7, and the reduction with respect to the original CC, shown in Figure 8, option A is the one that achieves the highest reduction in fuel consumption. From the original consumption of 3.42 kg/s, option A may save around 49% of the original fuel consumption if 35 MW of solar heat are added to the cycle, whereas option B can only reach around 21% savings. Nevertheless, it must not be forgotten that, although option A increases the cycle efficiency and reduces fuel consumption, the total net power delivered by the cycle is decreased with the integration of solar heat, as a consequence of the increase on the compressor power. Therefore, its use is not recommended. Option B does not have that disadvantage, as the integration of solar heat is performed after the compression stage. In addition, cycle efficiency increases more than with option A. Consequently, option B is the most adequate for integrating solar heat into the upper gas cycle of a CC.

https://doi.org/10.52202/069564-0055

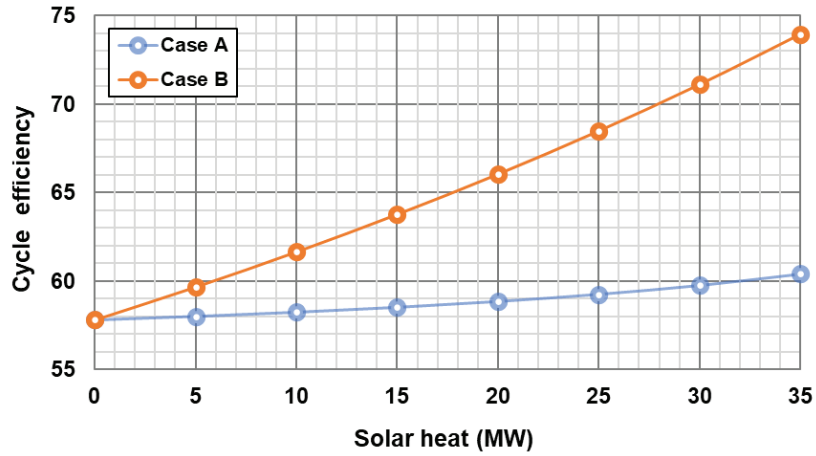

Figure 6: Combined cycle efficiency as a function of solar heat integrated into the cycle.

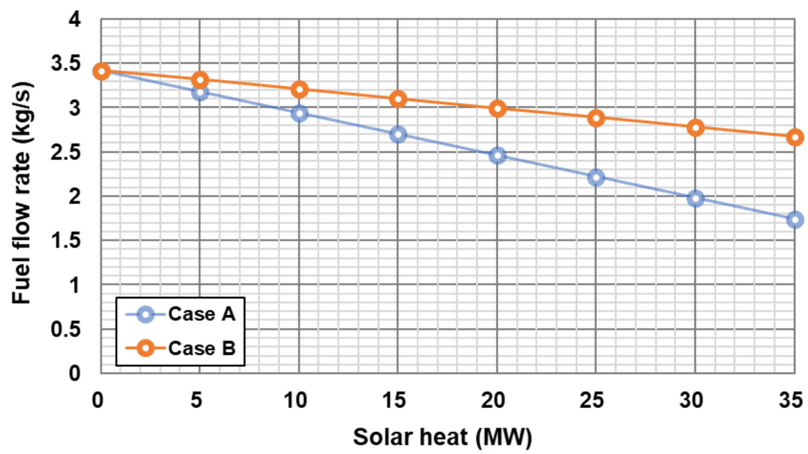

Figure 7: Fuel mass flow rate as a function of solar heat integrated into the cycle.

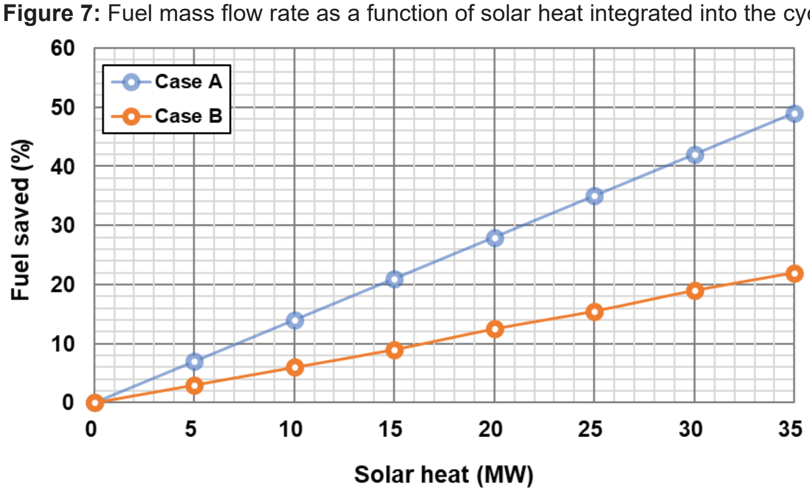

Figure 8: Fuel savings (%) as a function of solar heat integrated into the cycle.

Once it was been verified that option B is the most suitable one, in order to provide an estimation of the economic and environmental effects of solar heat integration, values from average solar irradiation in Las Palmas de Gran Canaria were considered. Figure 9 shows the monthly average daily global irradiation in Las Palmas, alongside the average heat power that could be provided by a 300,000 m^2 solar collector [29]. Maximum values of solar power are found in July, with 30,448 kW, while the minimum average solar heat is 15,597 kW, in December.

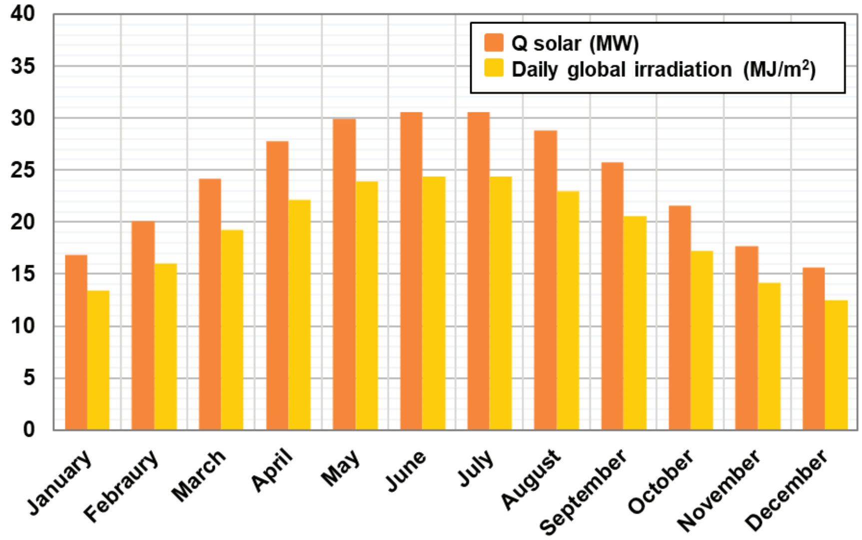

Figure 9: Monthly average daily global irradiation and solar heat power potential for a 300,000 m^2 collector in Las Palmas de Gran Canaria [29].

After the data from the solar heat power potential provided by the collector are introduced into the thermodynamic model of option B for the ISSC, the reduction in the fuel mass flow was calculated and translated into an estimation of the economic savings and reduction in CO_2 emissions. The results reveal a direct proportionality relation between the introduced solar heat power and the amount of fuel that may be saved. As shown in Figure 10, the highest savings may be achieved in July, of around 0.75 M€, while the lowest savings are reached in December, of around 0.38 M€. In all, if option B is integrated into the combined cycle, potential yearly savings of around 7.14 M€ might be achieved.

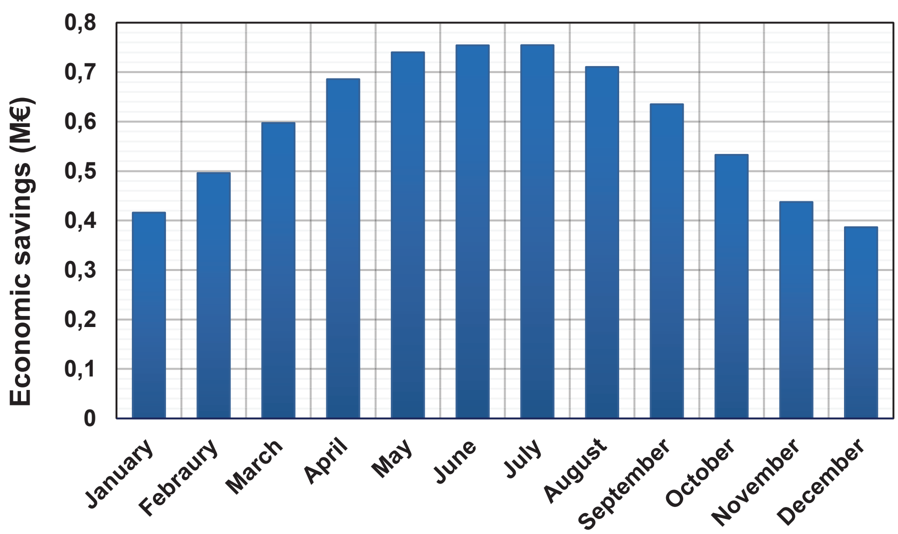

Figure 10: Monthly potential economic savings (M€) related to fuel consumption reduction.

Regarding the CO_2 emissions avoided by the integration of option B into the combined cycle, depicted in Figure 11, a direct proportionality with solar irradiance is found as well. Maximum values of potential reduction of emissions are found in July, of around 1.45 Mkg, whereas lowest values are found in December, of around 0.74 Mkg. In the aggregate, it has been estimated that incorporating option B into the combined cycle might lead to a total potential of reduction in CO_2 emissions of 13.75 Mkg per year.

https://doi.org/10.52202/069564-0055

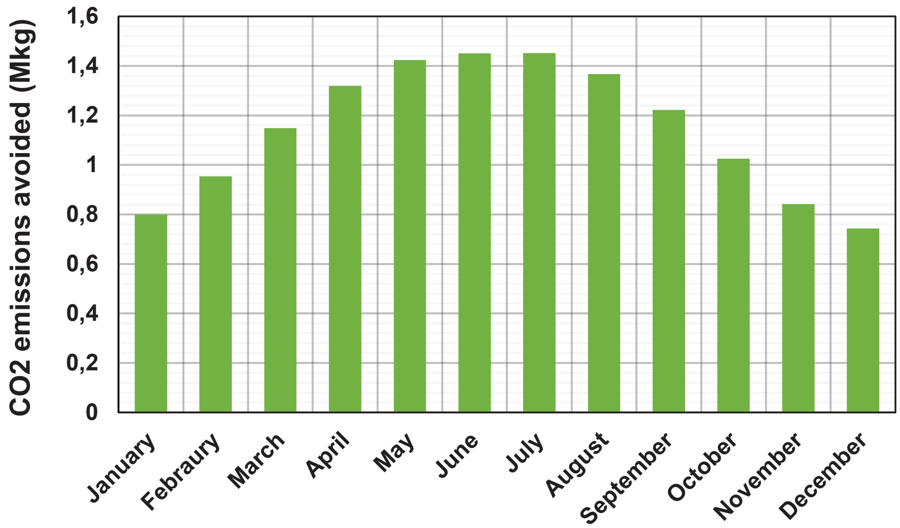

Figure 11: Monthly potential CO_2 emissions avoided (Mkg) related to fuel consumption reduction.

5. Conclusion

The overview of the power generation system in the Canary Islands reveals the important effect of renewable energy resources (especially, solar energy) to provide stability and reinforcement for power generation in thermal plants. The results from this work, which aims to evaluate the feasibility of integrating solar energy into a combined cycle power plant for fuel saving in insular subtropical climates, may contribute to improve the energy supply network in the Canary Islands, providing more energy security to the islands and reducing fuel imports. A thermodynamic model for solar heat integration into the upper gas cycle of the combined cycle was developed, studying the effects of injecting the solar heat before (case A) and after (case B) the compressor, before the combustion chamber.

It was found that the highest amount of fuel saved, 49% when injecting 35 MW of solar heat, was achieved when injecting the solar heat before the compressor (option A). However, this option resulted in a substantial increase of the compressor work due to the higher temperatures at the compressor inlet, reducing the net power of the cycle, although a global efficiency increase of around 2% was achieved. On the other hand, integrating the solar heat after the compressor (option B) had a very positive effect, with an overall 16.2% increase in the combined cycle efficiency when 35 MW of solar heat were introduced before the combustion chamber and. This option, in addition, can deliver the same net power with a substantial reduction of 22% in fuel consumption. The gap between the combined cycle efficiencies of both integration options became larger with the increase in the injected heat, with option B outperforming option A. Consequently, it may be argued that the most adequate for integrating solar heat into the upper gas cycle of a CC is right after the compressor and before the combustion chamber.

Combining the results from the energy analysis with the monthly solar irradiation distribution in Las Palmas de Gran Canaria and considering a solar collector of 300,000 m^2, it was possible to obtain an estimate of the economic savings and reduction in CO_2 emissions with the introduction of the solar field before the gas cycle combustion chamber. Oscillating between a minimum value of around 0.38 M€ in December and a maximum of 0.75 M€ in July, the integration of the proposed option may lead to potential savings of 7.14 M€ per year. Considering the CO_2 emissions potentially avoided with to the proposed solar heat integration, between 0.74 Mkg in December and 1.45 Mkg in July, it has been estimated that incorporating option B into the combined cycle might lead to a total potential of reduction in CO_2 emissions of 13.75 Mkg per year.

To conclude with, the integration of solar heat into a combined natural gas-fired cycle before the combustion chamber seems to be a very beneficial option for insular systems with solar irradiance values similar to Las Palmas de Gran Canaria. Substantial increases in the cycle efficiency, high potential economic savings, and a high reduction in potential CO_2 emissions are to be expected. Future works may focus on developing an exergoeconomic and environmental analysis of the studied alternatives, as well the study of other possible integration options of solar heat into the combined cycle.

Nomenclature

CC	Combined cycle
C_f	Fuel cost (€/kWh)
CSP	Concentrated solar power
DNI	Direct Normal Irradiance
$EF_{NG \rightarrow CO_2}$	Emission factor of natural gas (kg CO_2/kWh)
GEF	Global Environment Facility
GTCC	Gas turbine combined cycle
h_i	Specific enthalpy at state i (kJ/kg)
HRSG	Heat Recovery Steam Generator
ISCC	Integrated solar combined cycle power plant
LHV	Lower heating value (kJ/kg)
Mtoe	Million tonnes of oil equivalent
$\dot{m}_i$	Mass flow of fluid i (kg/s)
NGCC	Natural gas-fired combined cycle
PTC	Parabolic trough collectors
$\dot{Q}_i$	Heat transfer rate exchanged by component i (kW)
RES	Renewable energy sources
SEGS	Solar electric generating system
$\dot{W}_i$	Power of component i (kW)

Greek symbols

Δt	Time period (month)
η	Cycle efficiency

Subscripts

a	Air, case "A"
b	Case "B"
cc	Combustion chamber
CC	Combined cycle
$comp$	Compressor
f	Fuel
g	Gas
G	Gas cycle
GT	Gas turbine
new	New value (after solar integration)
ST	Steam turbine

References

[1] International energy agency (IEA), Global energy review 2021 <https://www.iea.org/>

[2] Our world in data, project of the Global change data lab (GCDL), <https://ourworldindata.org/>

[3] Bakos, G. C., and D. Parsa. "Technoeconomic assessment of an integrated solar combined cycle power plant in Greece using line-focus parabolic trough collectors." Renewable energy 60 (2013): 598-603.

[4] Behar, Omar, et al. "Instantaneous performance of the first integrated solar combined cycle system in Algeria." Energy Procedia 6 (2011): 185-193.

[5] Amelio, Mario, et al. "An evaluation of the performance of an integrated solar combined cycle plant provided with air-linear parabolic collectors." Energy 69 (2014): 742-748.

[6] Kabir, Ehsanul, et al. "Solar energy: Potential and future prospects." Renewable and Sustainable Energy Reviews 82 (2018): 894-900.

[7] Duffie, John A., William A. Beckman, and W. M. Worek. "Solar engineering of thermal processes." (1994): 67-68.

https://doi.org/10.52202/069564-0055

[8] Raafat, Samir W. Maadi 1904-1962: Society and history in a Cairo suburb. Palm Press, 1994.

[9] TB, Johansson, et al. Renewable Energy-Sources for Fuels and Electricity. 1993.

[10] Pilkington, S. "Solar International." Status Report on Solar Trough Power Plants, Pilkington Solar International GmbH, Germany (1996).

[11] The World Bank. Implementation Completion and Results Report (TF-91289) on A Grand in The Amount of US $49.80 Million to the Arab Republic of Egypt for the Kureimat Solar Thermal Hybrid Project; The World Bank: Washington, DC, USA, 2012.

[12] Allani, Yassine, Daniel Favrat, and M. R. Von Spakovsky. "CO2 mitigation through the use of hybrid solar-combined cycles." Energy conversion and management 38 (1997): S661-S667.

[13] Dersch, Jürgen, et al. "Trough integration into power plants—a study on the performance and economy of integrated solar combined cycle systems." Energy 29.5-6 (2004): 947-959.

[14] Franchini, Giuseppe, et al. "A comparative study between parabolic trough and solar tower technologies in Solar Rankine Cycle and Integrated Solar Combined Cycle plants." Solar Energy 98 (2013): 302-314.

[15] Antonanzas, J., et al. "Potential solar thermal integration in Spanish combined cycle gas turbines." Renewable and Sustainable Energy Reviews 37 (2014): 36-46.

[16] Li, Yuanyuan, and Yongping Yang. "Thermodynamic analysis of a novel integrated solar combined cycle." Applied energy 122 (2014): 133-142.

[17] Calise, Francesco, et al. "Thermoeconomic analysis of an integrated solar combined cycle power plant." Energy Conversion and Management 171 (2018): 1038-1051.

[18] Abdelhafidi, Nedjma, İbrahim Halil Yılmaz, and Nour El Islam Bachari. "An innovative dynamic model for an integrated solar combined cycle power plant under off-design conditions." Energy Conversion and Management 220 (2020): 113066.

[19] Temraz, Ayman, et al. "Development and Validation of a Dynamic Simulation Model for an Integrated Solar Combined Cycle Power Plant." Energies 14.11 (2021): 3304.

[20] Benabdellah, Hamza Moussa, and Adel Ghenaiet. "Energy, exergy, and economic analysis of an integrated solar combined cycle power plant." Engineering Reports 3.11 (2021): e12404.

[21] Zhang, Zuxian, et al. "General performance evaluation method of integrated solar combined cycle (ISCC) system." Energy 240 (2022): 122472.

[22] Lee, Taedong, Mark B. Glick, and Jae-Hyup Lee. "Island energy transition: Assessing Hawaii's multi-level, policy-driven approach." Renewable and Sustainable Energy Reviews 118 (2020): 109500.

[23] Daily characteristics of the Canary Islands' electricity system. Available at: <https://www.ree.es/en/balance-diario/canarias/2022/03/31>

[24] Canary Islands energy yearbook 2020. Available at: https://www.gobiernodecanarias.org/energia/publicaciones/

[25] Egyptian Petrochemicals Company (egy-petrochem.com)

[26] Energy price data and fuel price forecasts. Available at: <https://www.globalpetrolprices.com/>

[27] World Nuclear Association – Heat values of various fuels. Available at: <https://world-nuclear.org/information-library/facts-and-figures/heat-values-of-various-fuels.aspx>

[28] "Recognized Document of the Regulation of Thermal Installations in Buildings (RITE)" Joint resolution of the Ministries of Industry, Energy and Tourism, and the Ministry of Public Works. Available at: <https://energia.gob.es/desarrollo/EficienciaEnergetica/RITE/Reconocidos/Reconocidos/Otros%20documentos/Factores_emision_CO2.pdf>

[29] Technical guide to solar thermal energy provided by The Institute for Energy Diversification and Saving (IDAE) and the Solar Thermal Industry Association (ASIT), organizations affiliated with the European Union. Available at: <https://www.idae.es/publicaciones/guia-tecnica-de-energia-solar-termica>